

# Thermodynamic Analysis of the Process Obtaining Promoted Iron in Various Gaseous Media



L. Frolova and B. Blyuss

**Abstract** A thermodynamic analysis of the reduction process of iron-based oxide systems with nickel and cobalt additives in various gaseous media (coke oven gas, carbon monoxide(II), and hydrogen) has been carried out. The method of minimizing the total thermodynamic potentials was used to calculate the equilibrium compositions of the products of the process under study. The expediency of using hydrogen for the reduction of iron oxide is shown. Its optimal concentration and process temperature are established.

**Keywords** Iron oxide · Reduction · Gas media · Thermodynamics

## 1 Introduction

Currently, the areas of use of nanodispersed metals and alloys are expanding, including in environmental technologies [1–5]. One of these materials is nanocomposites based on nanoiron, which have high catalytic and adsorption characteristics in the purification of aqueous media from organic and inorganic contaminants and high magnetic characteristics [6]. The efficiency of using such materials is associated with the high dispersion of iron nanoparticles and, accordingly, their large specific surface area and chemical activity. Despite many advantages, such systems have a number of disadvantages, the main of which is significant pyrophoricity, the tendency of particles to aggregate. One way to slow down these processes is doping nanoiron particles with transition metal cations and synthesizing composites [7–9]. Therefore, the presence of cobalt and nickel stabilizes nanosized iron. Thus, the relevance of the work is pre-determined by the need to improve modern highly efficient photocatalysts, catalysts, and adsorbents. There are various technologies for obtaining dispersed iron. For example, the decomposition of  $\text{Fe}(\text{CO})_5$  in organic solvents or in argon. But the most common method is the reduction of  $\text{Fe}^{2+}$  or  $\text{Fe}^{3+}$  ions from solutions of their salts with alkali metal borohydrides [10, 11]. The iron obtained

---

L. Frolova (✉) · B. Blyuss  
Ukrainian State University of Chemical Technology, Dnipro, Ukraine  
e-mail: [19kozak83@gmail.com](mailto:19kozak83@gmail.com)

© The Author(s), under exclusive license to Springer Nature Switzerland AG 2023  
O. Fesenko and L. Yatsenko (eds.), *Nanomaterials and Nanocomposites, Nanostructure Surfaces, and Their Applications*, Springer Proceedings in Physics 279,  
[https://doi.org/10.1007/978-3-031-18096-5\\_3](https://doi.org/10.1007/978-3-031-18096-5_3)

in this way has a typical so-called “core–shell” structure in which the central part consists of iron, and the surface is covered with a thin layer of Fe(II) and Fe(III) oxides, which are formed as a result of oxidative processes. These materials have a large specific surface area and high reactivity. However, a significant disadvantage is that nanoiron has a tendency to aggregate and is easily oxidized with the formation of an oxide layer on the particle surface. These factors reduce the activity and efficiency of nanoiron [12].

The most common variant of the technology for producing iron powder is the reduction of iron oxides and hydroxides ( $\text{Fe}_2\text{O}_3$ ,  $\text{Fe}_3\text{O}_4$ ,  $\text{Fe}(\text{OH})_3$ , and  $\alpha\text{-FeOOH}$ ) with hydrogen [13–15]. In this case, the metal particles mainly retain the shape and particle size distribution of the original powder during the reduction process under certain conditions.

The same group of methods includes obtaining oxides through carbonate, oxalate, oxyhydroxides (goethite, lepidocrocite), or other insoluble but easily decomposing compounds. The main advantage of these methods is the possibility of obtaining a pure product even when raw materials of low purity are used.

By calcining powders of coagulated Ni- and Fe-tartrates at 250–400 °C (2 h), ultra-fine Ni(II) ferrite powders with a particle size of 10 nm were obtained. In powders, mixtures of Ni- and Fe-tartrates have the chemical properties of individual salts. The homogeneity of their mixing strongly affects the course of the thermal reaction and the properties of the resulting powders. The reservoir temperature and particle size increase with the deterioration of mixing, which initiates an increase in the size of intermediate phases ( $\alpha\text{-Fe}_2\text{O}_3$ , NiO, or Ni) [16].

The general scheme for obtaining highly dispersed iron powder can be represented as follows:

- production of hydroxides
- dehydration of hydroxides to oxides
- reduction of oxides to metallic iron.

In this case, the size and shape of powder particles are mainly determined by the structure of hydroxides.

The reduction process is the final stage and largely determines the important parameters such as the granulometric composition of products, the content of metallic iron in them, and the structure of particles [17–19]. These parameters can be significantly affected by the choice of reducing gas, since it determines the temperature regime of the process, the composition of the gaseous medium, and, consequently, the state of the surface of the final product [20].

It is known that the reduction and regeneration of iron oxides can be carried out not only with hydrogen, carbon monoxide, and ammonia, but also with technically available gas mixtures: coke, generator, water, etc.

## 2 Methodology

For reasonable choice of the optimal gas medium, a thermodynamic analysis of the reduction process was carried out.

Thermodynamic calculations were carried out according to the method, which is based on the first variational principle of chemical thermodynamics, using the ASTRA program.

On the basis of thermodynamic calculations, the equilibrium compositions of the products of chemical reactions were determined at various initial compositions, temperatures, and pressures.

The powder with the optimal weight content of the components was taken as the feedstock. In terms of oxides in wt %:  $\text{Fe}_2\text{O}_3$ –95, NiO–4, and CoO–1.

Coke oven gas based on, (composition: 57%  $\text{CH}_4$ , 34%  $\text{H}_2$ , 3% CO, 4.4% ( $\text{CO}_2 + \text{N}_2$ ), 0.4  $\text{O}_2$ , 1.2% heavy hydrocarbons), CO and hydrogen. The amounts of gases were taken in excess of the stoichiometric amount.

The calculation was carried out in the temperature range 300–1100 K at a pressure of 0.1 MPa. During the calculation, the influence of the composition of the reducing gaseous medium on the course of the process was studied. The calculation was carried out taking into account the possibility of formation of the following products:  $\text{Fe}_2\text{O}_3$ ,  $\text{Fe}_3\text{O}_4$ , FeO, CoO, NiO, Fe, C,  $\text{Fe}_3\text{C}$ , Co, and Ni in the condensed phase and H,  $\text{H}_2$ ,  $\text{H}_2\text{O}$ ,  $\text{NH}_3$ , CO,  $\text{CO}_2$ ,  $\text{CH}_4$ ,  $\text{CH}_3$ ,  $\text{C}_2\text{H}_2$ ,  $\text{C}_6\text{H}_6$ ,  $\text{CH}_2\text{O}$ ,  $\text{N}_2\text{C}$ , and HCN in the gas phase. The concentrations of substances were expressed in mol/kg of the system under study.

## 3 Results and Its Discussion

The temperature dependence of the equilibrium composition of the  $\text{Fe}_2\text{O}_3$ –CoO–NiO oxide system during reduction with coconut gas is shown in Fig. 1.

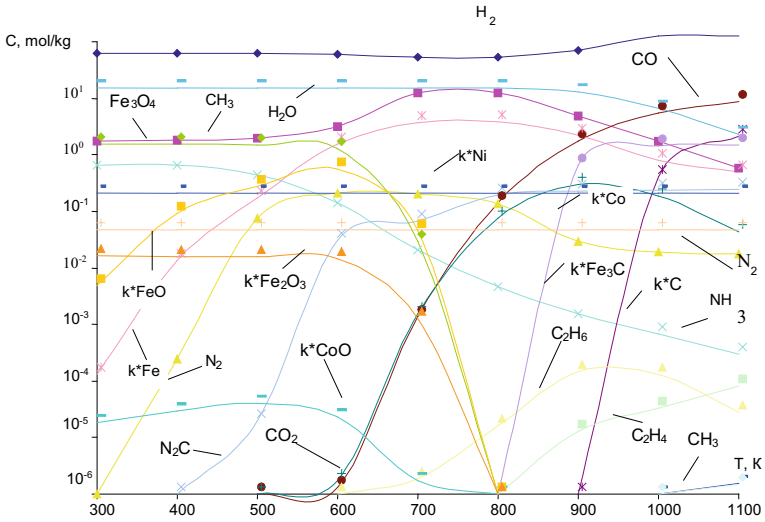
From the analysis of the dependence, it follows that the complete reduction of iron oxides to metal occurs at 700 K, and with a further increase in temperature, its amount decreases due to the formation of iron carbide. Nickel oxides are completely reduced at 400 K and cobalt at 900 K.

Figure 2 shows the temperature dependence of the equilibrium compositions of the same system during the reduction of carbon monoxide(II).

As can be seen from Fig. 2, the reduction of oxides begins at 500 K; however, the degree of reduction strongly depends on temperature and is maximum at 1000 K.

Nickel oxide is reduced at 400 K and cobalt oxide at 800 K. At 900 K, the existence of iron carbide is thermodynamically possible. The reducing properties of the released carbon appear at a temperature of 1000 K.

Figure 3 shows the results of thermodynamic calculations of the chemisorbent reduction process in a hydrogen medium. Nickel oxide is completely reduced to metal at 400 K, at 600 K oxides of iron and cobalt.



**Fig. 1** Dependence of the equilibrium composition of the Fe-Co-Ni-C-N-O-H system on temperature during reduction with coke oven gas, pressure 0.1 MPa

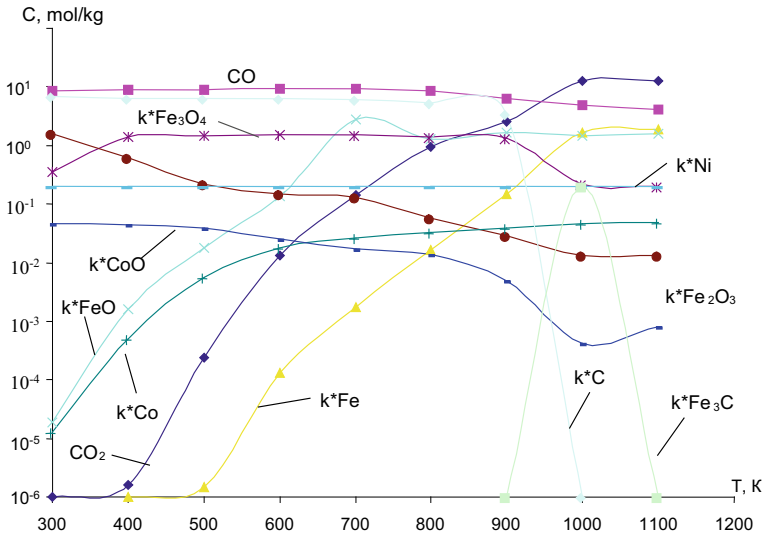


**Fig. 2** Dependence of the equilibrium composition of the Fe-Co-Ni-C-N-O-H system on temperature during CO reduction, pressure 0.1 MPa

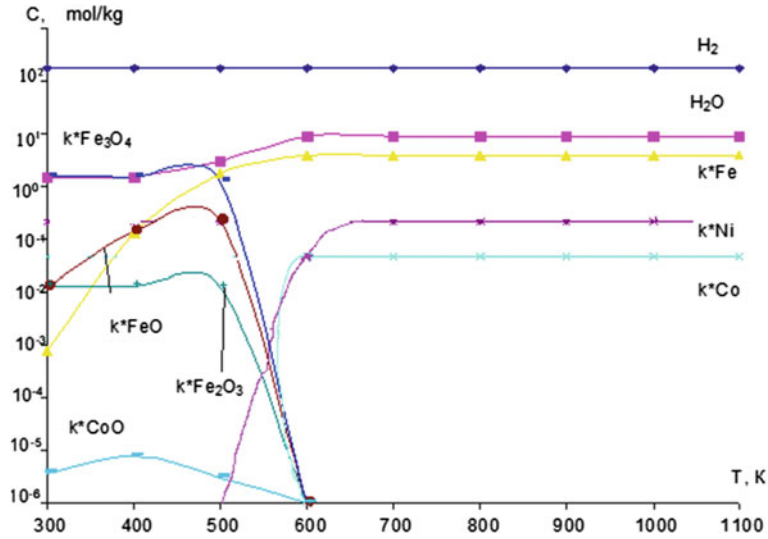
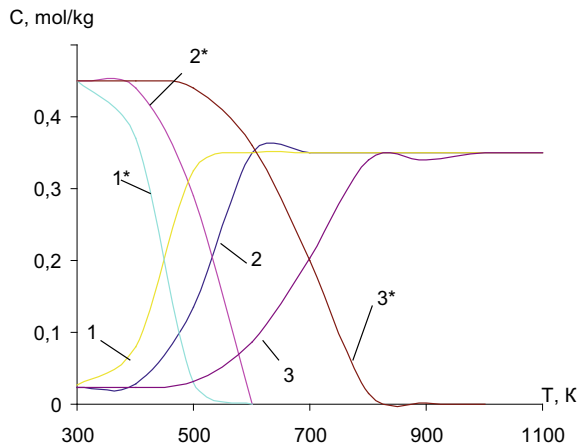


**Fig. 3** Dependence of the equilibrium composition of the Fe–Co–Ni–O–H system on temperature during hydrogen reduction, pressure 0.1 MPa

To clarify the optimal hydrogen concentrations, which allow the reduction of the complex Fe–Co–Ni oxide system at lower temperatures, the influence of the hydrogen content in the gas mixture on the temperature of the complete reduction of oxides was studied.

Figure 4 shows the generalized temperature dependence of the total concentrations of two solid phases. The first contains metal oxides, and the second contains metals at different hydrogen concentrations.

**Fig. 4** Dependence of the total concentrations of the solid phase of the Fe–Co–Ni–C–N–O–H system on temperature at  $P = 0.1$  MPa, the gaseous medium is hydrogen; 1–3—total concentration of metals; 1\*–3\*—total concentration of metal oxides; 1–1\*—90%  $H_2$ , 2–2\*—60%  $H_2$ , and 3–3\*—20%  $H_2$



Comparing the presented results, we can conclude that with an increase in the hydrogen content in the gas mixture, the temperature region of the existence of a solid solution of iron, cobalt, and nickel increases, and the temperature of the complete reduction of oxides shifts to lower temperatures.

According to the results obtained from thermodynamic calculations, hydrogen is the optimal gas medium, since it provides complete reduction of iron, cobalt, and nickel oxides to metals at 600 K (hydrogen concentration 60% wt.), while the product is not cracked by carbon and iron carbide. Thus, the highly developed porous surface of the catalyst, the structure of the particles, and, as a result, the good adsorption capacity of the metal powder are preserved.

## References

1. Tanwar R, Kumar S, Mandal UK (2017) Photocatalytic activity of PANI/Fe<sup>0</sup> doped BiOCl under visible light-degradation of Congo red dye. *J Photochem Photobiol A: Chem* 333:105–116
2. Zhou M et al (2005) Preparation and photocatalytic activity of Fe-doped mesoporous titanium dioxide nanocrystalline photocatalysts. *Mater Chem Phys* 93(1):159–163
3. Hu B et al (2018) Co/Fe-bimetallic organic framework-derived carbon-incorporated cobalt–ferric mixed metal phosphide as a highly efficient photocatalyst under visible light. *J Colloid Interface Sci* 531:148–159
4. Till BA, Weathers LJ, Alvarez PJJ (1998) Fe(0)-supported autotrophic denitrification. *Environ Sci Technol* 32(5):634–639
5. Cheng R, Wang J, Zhang W (2007) Comparison of reductive dechlorination of p-chlorophenol using Fe<sup>0</sup> and nanosized Fe<sup>0</sup>. *J Hazard Mater* 144(1–2):334–339
6. Son HS, Im JK, Zoh KD (2009) A Fenton-like degradation mechanism for 1, 4-dioxane using zero-valent iron (Fe<sup>0</sup>) and UV light. *Water Res* 43(5):1457–1463
7. Scorzelli RB (1997) A study of phase stability in invar Fe–Ni alloys obtained by non-conventional methods. *Hyperfine Interact* 110(1):143–150
8. Yao LH et al (2010) Core–shell structured nanoparticles (M@ SiO<sub>2</sub>, Al<sub>2</sub>O<sub>3</sub>, MgO; M= Fe, Co, Ni, Ru) and their application in CO<sub>x</sub>-free H<sub>2</sub> production via NH<sub>3</sub> decomposition. *Catal Today* 158(3–4):401–408
9. Frolova L, Kharytonov M (2019) Synthesis of magnetic biochar for efficient removal of Cr(III) cations from the aqueous medium. *Adv Mater Sci Eng* 2019
10. Nguyen TH et al (2021) Impact of iron on the Fe–Co–Ni ternary nanocomposites structural and magnetic features obtained via chemical precipitation followed by reduction process for various magnetically coupled devices applications. *Nanomaterials* 11(2):341
11. Bilgiliyoy E et al (2021) Low energy electron- and ion-induced surface reactions of Fe(CO)<sub>5</sub> thin films. *J Phys Chem C* 125(32):17749–17760
12. Kwak YJ, Park HR, Song MY (2017) Analysis of the metal hydride decomposition temperatures of Zn(BH<sub>4</sub>)<sub>2</sub>–MgH<sub>2</sub>–Tm (Tm = Ni, Ti or Fe) using a sievert's type volumetric apparatus. *Mater Sci* 23(1):21–26
13. Toneguzzo P et al (2000) CoNi and FeCoNi fine particles prepared by the polyol process: physico-chemical characterization and dynamic magnetic properties. *J Mater Sci* 35(15):3767–3784
14. Frolova LA, Hrydnieva TV (2020) Influence of various factors on the ferric oxyhydroxide synthesis. *J Chem Technol* 28(1):61–67
15. Frolova LA, Khmelenko OV (2021) The study of Co–Ni–Mn ferrites for the catalytic decomposition of 4-nitrophenol. *Catal Lett* 151(5):1522–1533

16. Wang D et al (2017) Innovative evaluation of CO-H<sub>2</sub> interaction during gaseous wustite reduction controlled by external gas diffusion. *Int J Hydrogen Energy* 42(20):14047–14057
17. Yang JM, Tsuo WJ, Yen FS (1999) Preparation of ultrafine nickel ferrite powders using mixed Ni and Fe tartrates. *J Solid State Chem* 145(1):50–57
18. Orth WS, Gillham RW (1995) Dechlorination of trichloroethene in aqueous solution using Fe<sup>0</sup>. *Environ Sci Technol* 30(1):66–71
19. Geng B et al (2009) Kinetics of hexavalent chromium removal from water by chitosan-Fe<sup>0</sup> nanoparticles. *Chemosphere* 75(6):825–830
20. Mikhailichenko AI, Nefedova NV, Karateeva EY (1998) Hydrogen reduction of ultrafine α-Fe<sub>2</sub>O<sub>3</sub> powders. *Russ J Inorg Chem* 43(2):138–141